11.5 RESULTS OF USING THE PSU SHALLOW CONVECTION SCHEME IN AN ENSEMBLE MODE: EFFECTS ON THE MASS FLUX PROFILES AND THERMODYNAMIC TENDENCIES

Ricardo C. Muñoz*, Nelson L. Seaman, David R. Stauffer, Aijun Deng
Department of Meteorology
The Pennsylvania State University
University Park, PA

1. INTRODUCTION

The rapid increase in computing power available today means that meteorological models can be run with greater vertical and horizontal resolutions. However, for certain problems such as understanding regional-scale atmospheric water budgets, finer grid resolutions need to be accompanied by more realistic physical parameterizations. In this case it is especially important to improve the treatment of shallow cumulus convection in global scale and mesoscale models.

More physically realistic parameterizations usually are also more complex and involve a larger number of parameters. Considerable effort is needed to calibrate these schemes and validate them for a range of applications. In this paper we describe sensitivities and improvements made to the Penn State Univ. (PSU) shallow convection parameterization developed by Deng (1999) and described by Deng et al. (2002). Muñoz et al. (2001) applied this scheme in the 3-D MM5 model to simulate summertime shallow convection over the central U.S. While the results were encouraging because the shallow convection scheme was able to capture much of the spatial distribution of shallow clouds, systematic under-prediction of cloud fraction was also found and cloud fields exhibited unrealistic patchiness.

2. OVERVIEW OF PSU SHALLOW CONVECTION

The PSU shallow convection scheme can be considered an extension of the Kain-Fritsch (KF) (1990) deep convection parameterization adapted for shallow non-precipitating clouds. As for deep convection schemes, the PSU shallow convection scheme contains a triggering condition, a cloud model and a closure assumption. However, the representation of shallow clouds in mesoscale models poses some problems that are not as relevant in the deep convection case. For example, it is important to call the parameterization more often than for the deep convection schemes, since shallow clouds interact more rapidly with the other model physics, especially the land surface, turbulence and radiative parameterizations. Also, shallow clouds tend to have much smaller thermodynamic perturbations as compared with deep convection. Thus, the definition of the initial properties of an updraft parcel becomes a very sensitive part of the parameterization. Updraft and mixing algorithms proven useful in the parameterization of deep convection must be re-evaluated for the more subtle conditions of shallow convection, where buoyancy or liquid water content of the updraft may differ only marginally from those of the environment. A unique feature of the PSU shallow convection scheme is its treatment of the liquid water generated in the updraft. In the KF scheme, detrained liquid water is fed back immediately to the resolved water variables. However, the PSU shallow cloud scheme retains detrained condensed water as subgrid cloud fraction and subgrid liquid water content that are gradually put back into the resolved variables by means of mixing and other parameterized processes (Deng et al. 2002).

* Corresponding author: Ricardo C. Muñoz, 503 Walker Bldg., Dept. of Meteor., Penn State Univ, University Park, PA, 16802. Email: ricardo@essc.psu.edu

3. REVISIONS TO PSU CONVECTION SCHEME

3.1 *PARCEL PROPERTIES*

The original shallow convection scheme defined the thermodynamic properties of the updraft-initiating parcel based on the average properties of the lowest 20% of the planetary boundary layer (PBL). However, since those average PBL properties evolve slowly, updraft characteristics also change slowly. As will be shown later, more realistic convective mass flux profiles are obtained if the initial parcel properties are allowed to vary according to a prescribed probability distribution function. In the results presented here initial parcel temperature, T_p, and water mixing ratio, q_p, are defined respectively by $T_p = T_e + dt_r$ and $q_p = q_e + dq_r$, where the subscript 'e' denotes the environmental variable at the PBL top. The terms dt_r and dq_r correspond to random perturbations that are calculated with a binormal distribution function having means DT and DQ, standard deviations s_t and s_q, and correlation coefficient r_{tq}. Also, the initial parcel is not allowed to have a water content larger than saturation.

3.2 *VERTICAL CONTINUITY OF UPDRAFT MODEL*

The random variation of initial updraft properties (Sec. 3.1) introduces variability in the updraft top, mass fluxes, entrainment and detrainment profiles, etc. However, it was found that numerical and algorithmic artifacts in the original shallow convection scheme also could produce spurious and unrealistic fluctuations in the updrafts, even when the initial parcel properties did not change abruptly. A primary cause of this behavior is that the KF updraft model originally used in the shallow scheme discretized the updraft according to the vertical grid of the calling model. As a result, updraft mass flux could change abruptly by as much as 50% in one time

step when the top of the updraft rose suddenly to the next layer. These discretization problems are not very important for the KF updraft model because the deep convection tendencies are held constant for ~30 minutes.

The solution is to make the updraft algorithm able to recognize when a given model layer includes a significant transition level. The latter is defined as a level where 1) buoyancy changes sign, 2) liquid water becomes positive, 3) buoyant energy becomes zero, or 4) the updraft mass flux becomes zero. In these cases, the algorithm iterates inside the model layer to find the exact transition level. The logic of the new algorithm is somewhat more complex than in the original scheme, but it allows updrafts to evolve more smoothly.

3.3 *ENTRAINMENT/DETRAINMENT (ED) SCHEME*

A physically appealing algorithm in KF is used to diagnose the partitioning between updraft entrainment and detrainment. The scheme considers fractional mixtures of updraft and environmental air and calculates their resulting virtual temperatures. The mixing fraction with the same virtual temperature as the environment is called the critical mixing fraction, X_c. The entrainment/detrainment (ED) ratio increases with X_c.

The KF ED algorithm works reasonably well for deep convection where the thermodynamic perturbations of the updrafts are large. However, shallow convection tends to exhibit more subtle perturbations. In our tests we found that for parcels with small buoyancy excess a very small liquid water content is enough to make the updraft to detrain completely. As a result, the original ED algorithm can produce unrealistic mass flux profiles characterized by a rather shallow entrainment layer near updraft base topped by a deep detrainment layer aloft. We have tested a modified ED algorithm in which, as the liquid water content goes to zero, it is simply the updraft buoyancy that controls the entrainment/detrainment partitioning. Details of the new ED algorithm are fully described in Muñoz (2002).

3.4 *DETRAINMENT LAYER*

Like the original KF updraft model, the shallow-cloud updraft is forced to detrain when it becomes non-buoyant. The fractional amount of mass detrained, however, is made here proportional to the fraction of buoyant energy lost in the layer relative to the buoyant energy that the updraft parcel has at the layer base. In this way we make sure that the updraft mass flux goes to zero at the same rate at which the buoyant energy of the updraft parcel goes to zero (transition levels type 3 and 4 occur at the same height). This modification significantly affects the shape of the detrainment profile, and is partially responsible for shifting the detrainment peak downward near the updraft base where most of the initially non-buoyant parcels are forced to detrain.

3.5 *CLOSURE*

The closure of the original shallow convection scheme relates cloud base mass flux to the turbulence kinetic energy (TKE) in the PBL. We have extended this closure to allow the base mass flux to be a function of the energetics of the updraft. Thus, the more energetic the updraft-initiating parcel, the greater will be the cloud base mass flux. Details appear in Muñoz (2002).

3.6 *THERMODYNAMIC TENDENCIES IN THE PBL*

Finally, the convective mass flux is rooted in the PBL, and therefore it induces thermodynamic tendencies in the PBL. However, little is known about the vertical distribution of these tendencies and any change in the vertical distribution can significantly alter the evolution of the PBL. Thus, the simple approach of using a uniform vertical distribution for these tendencies has been taken. By doing so, we allow shallow convection to affect the evolution of the mean PBL temperature and water vapor, but not their vertical gradients.

4. MODEL SETUP

We have implemented and tested the modified shallow convection scheme in a 1-D version of the MM5 model. For these tests, surface fluxes, horizontal advection, subsidence and radiative forcing tendencies are all prescribed. Only the model's 1.5-order TKE-predicting turbulence scheme (Shafran et al. 2000) and the shallow cloud scheme are active. The 1-D model is run with 32 layers in the vertical. The shallow convection scheme is switched on two hours after the start of the run so that the TKE in the PBL has had time to develop.

5. *RESULTS FOR THE BOMEX CASE*

For the calibration and sensitivity analysis of the modified PSU shallow convection parameterization we use a trade-wind boundary layer case described by Siebesma and Cuijpers (1995) (SC95). They compared observed mass flux profiles and thermodynamic tendencies to LES results for the last 4 h of a 7-h simulation during an undisturbed period of the BOMEX experiment. We use the same initial sounding and forcings. One of the main conclusions in SC95 is that, compared to LES results, current mass flux parameterizations appear to underestimate mixing between updrafts and their environment by an order of magnitude.

Figure 1 illustrates our implementation of the ensemble of updraft-initiating parcel properties. Panel a) of the figure shows three time series of temperature. The dotted line is the environmental temperature at the PBL top, the circles give the temperature of the bottom 20 % of the PBL (translated adiabatically to the PBL top), and finally the continuous rapidly varying line traces the temperature used in each time step to define the initial updraft parcel. In this case the (potential) temperature variation in the PBL is very small, so we have assumed

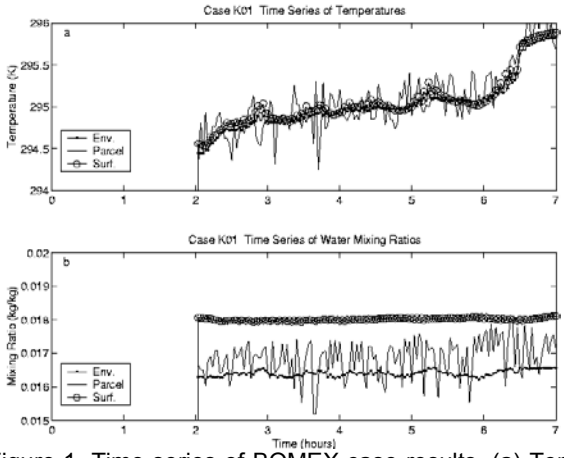

Figure 1. Time series of BOMEX case results. (a) Temperature at the updraft release height for the environment (dots), initial updraft parcel (continuous) and surface (adiabatically translated to release height) (circles). (b) Water vapor mixing ratio at release height for the environment (dots), initial parcel (continuous) and surface (circles).

DT=0.05 K and s_t =0.2 K. Panel b) is the corresponding information for water vapor mixing ratio. The vertical variation in mixing ratio across the PBL is much larger than for temperature, and we have used DQ=0.5 g/kg, and s_q =0.7 g/kg. The apparent asymmetry in the mixing ratio fluctuations is due to imposition of the saturation restriction on the initial parcels. The correlation between temperature and water vapor perturbations, r_{tq} , has been set to zero in these preliminary runs.

Figure 2a shows time series of the maximum predicted sub-grid cloud fraction. Soon after the shallow convection scheme is turned on, the cloud field moves toward equilibrium with cloud fractions between 10- 20% that compare well with results of SC95. Figure 2b shows the evolution of maximum relative humidity in the column (at the top of the PBL). The relative humidity at the PBL top stays around 95% in the first 4 h after the shallow convection was turned on, with a slight decreasing trend that accelerates at the end of the period. Other runs (not shown) indicate that the relative humidity at the top of the PBL is rather sensitive to the magnitude of the cloud base mass flux and the assumed mean thermodynamic properties of the initial cloud updrafts.

A better test of how well the shallow convection scheme is working is to compare the mass fluxes and convective thermodynamic tendencies produced by the parameterization to observations and/or LES results. Figure 3 shows mass flux profiles obtained with the scheme averaged for the last 4 h of simulation. These compare quite well with the corresponding vertical profiles presented by SC95 (Figure 4). The locations and magnitudes of the peaks in the profiles, the rapidly decreasing entrainment rate above its peak near cloud base and the more slowly decreasing detrainment profile are consistent with the LES results. We note that the cloud layer base in Fig. 3 is about 100 m lower than observed in BOMEX (Fig. 4), possibly due to a deficit in the sub-cloud turbulence.

Also, Fig. 3 shows mass flux profiles obtained with a selection of parameters that attempts to reproduce the original shallow convection scheme (dashed lines). That is, no variability is allowed in the initial updraft parcel and the original ED formulation is used. It is evident that this experiment fails to produce simultaneously significant entrainment and detrainment near cloud base, so that the profiles have little resemblance to those of the revised scheme and the LES results.

Finally, Figure 5a shows our vertical distribution of cloud area fraction and TKE. The former peaks at about 1000 m above the surface. The TKE peaks near the surface at about 0.12 J/kg. Figures 5b and c show respectively time-averaged tendency profiles for temperature and water vapor mixing ratio. The circles give the imposed forcings and the dotted lines give combined tendencies for TKE and the shallow

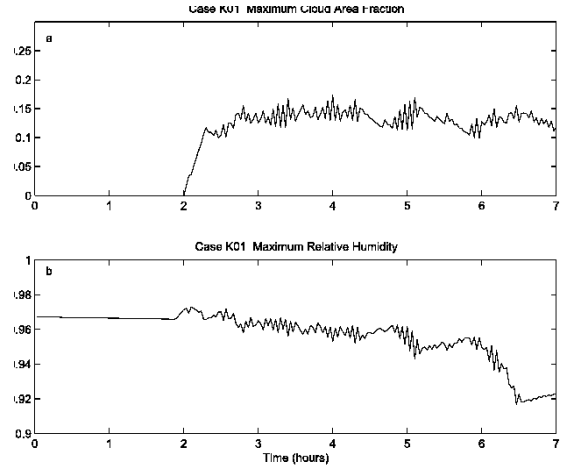

Figure 2. Time series of (a) column maximum cloud area fraction and (b) column maximum relative humidity.

convection. The vertical profiles for the convective thermodynamic tendencies agree in general terms with the corresponding profiles in SC95 (not shown), in which the cloud layer is warmed in its bottom half and cooled in the top where detrainment dominates. Also, a general moistening of the cloud layer by shallow convection is evident. The most important difference between these results and those in the SC95 is the level at which the detrainment thermodynamic tendencies peak. In our results this level is ~2000 m above the surface, while in SC95, it occurs ~1600 m. Also, near cloud base the current parameterization induces net drying that is not observed in the LES results. Further study is needed to understand these differences.

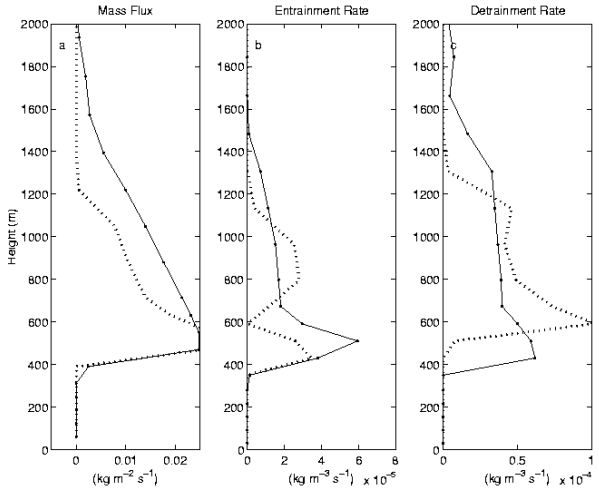

Figure 3. Averaged convective mass flux profiles calculated over 3-7 h. Solid-dotted lines show results using new algorithms in the shallow convection scheme. Dashed lines show results with a choice of parameters that approximates the original algorithms of the scheme. (a) Mass flux, (b) entrainment rate, (c) detrainment rate.

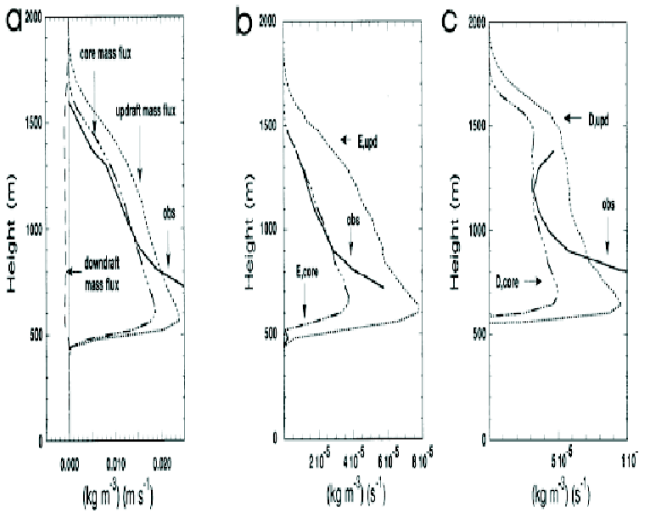

Figure 4. Mass flux profiles for BOMEX trade wind case. (a) Mass flux profile, (b) Entrainment rate profile, (c) Detrainment rate profile. Bold lines are profiles derived from observations, and the other two lines are derived from LES results with two methods of defining updrafts (after Siebesma and Cuijpers 1995).

6. CONCLUSIONS

The PSU shallow convection scheme, developed originally with a single cloud size, has been extended to consider an ensemble of clouds by varying the properties of the initiating cloud parcels according to a probability distribution. This has required among other things revisions to the standard KF updraft algorithm to make sure that it behaves smoothly for smooth variations in the properties of its initiating parcels. In one-dimensional tests using a BOMEX initial profile, results show that the ensemble of clouds produces realistic profiles (magnitudes & shapes) for entrainment/detrainment, total mass flux, and thermodynamic tendencies when compared with observations and LES results.

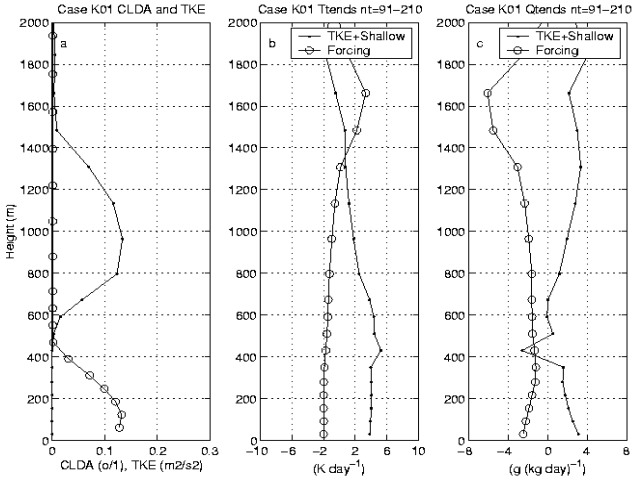

Figure 5. Average vertical profiles for (a) cloud area fraction (dots) and TKE (circles), (b) temperature tendencies of the forcing (circles) and sum of turbulent and convective tendencies (dots), (c) water vapor mixing ratio tendencies of the forcing (circles) and the sum of turbulent and convective tendencies (dots).

7. REFERENCES

Deng, A. 1999: A shallow-convection parameterization scheme for mesoscale models. Ph.D. Thesis, Dept. of Meteorology, The Pennsylvania State University, 152 pp.

Deng, A., N.L. Seaman and J.S. Kain, 2002: A shallow-convection parameterization for mesoscale models. Part I Sub-model description and preliminary applications. *J. Atmos. Sci.*, **59**, accepted for publication, 56 pp.

Kain, J.S. and J.M Fritsch, 1990: A one-dimensional entraining/detraining plume model and its application in convective parameterization. *J. Atmos. Sci.*, **47**, 2784-2802.

Muñoz, R.C., 2002: Development and testing of physical sub-grid parameterizations for the study of shallow convection interactions over land. Ph.D. thesis, Dept. of Meteorology, The Pennsylvania State Univ., in preparation.

Muñoz, R.C., N.L. Seaman, D.R. Stauffer, and A. Deng, 2001: Modeling the interaction between boundary layer and shallow clouds using a TKE and a shallow con-vection parameterization. 9th AMS Conf. on Mesoscale Processes, 26-30.

Siebesma, A.P., and J.W.M. Cuijpers, 1995: Evaluation of parametric assumptions for shallow convection. J. Atmos. Sci., 52, 650-666.